Spatially resolved gap closing in single Josephson junctions constructed on Bi_2Te_3 surface*

Yuan Pang(庞远)[1], Junhua Wang(王骏华)[1], Zhaozheng Lyu(吕昭征)[1], Guang Yang(杨光)[1], Jie Fan(樊洁)[1], Guangtong Liu(刘广同)[1], Zhongqing Ji(姬忠庆)[1], Xiunian Jing(景秀年)[1,2], Changli Yang(杨昌黎)[1,2], and Li Lu(吕力)[1,2,†]

[1] *Beijing National Laboratory for Condensed Matter Physics, Institute of Physics, Chinese Academy of Sciences, Beijing* 100190, *China*
[2] *Collaborative Innovation Center of Quantum Matter, Beijing* 100871, *China*

(Received 11 April 2016; revised manuscript received 10 May 2016; published online 30 September 2016)

Full gap closing is a prerequisite for hosting Majorana zero modes in Josephson junctions on the surface of topological insulators. Previously, we have observed direct experimental evidence of gap closing in Josephson junctions constructed on Bi_2Te_3 surface. In this paper we report further investigations on the position dependence of gap closing as a function of magnetic flux in single Josephson junctions constructed on Bi_2Te_3 surface.

Keywords: topological insulator, proximity effect, Josephson junction, Majorana zero mode

PACS: 74.45.+c, 03.65.Vf, 71.70.Ej, 73.40.–c **DOI:** 10.1088/1674-1056/25/11/117402

1. Introduction

It is predicted that Majorana zero modes can be produced in condensed matter systems.[1–8] To search for Majorana zero modes, various experiments have been carried out on topological insulator (TI) or related, material-based devices, reporting the observation of, for examples, a zero bias conductance peak (ZBCP),[9–16] and a component of 4π-periodic current-phase relations.[17–23] However, so far there is still a lack of a consensus that Majorana fermions have been found. More experimental evidence is still needed to fully confirm the existence of Majorana zero modes.

For S–TI–S type Josephson junctions (where S denotes *s*-wave superconductor), the Andreev reflection of helical electrons on the TI surface is topologically protected to be fully transparent. When the phase difference of the junction reaches π, the two lowest-energy branches of Andreev bound states cross with each other at the fermi level, resulting in the closing of the minigap[7,24] and thus the formation of 4π-periodic energy-phase relations (EPRs).[25–32] Previously, we have already observed gap closing and 2π-periodic but fully skewed EPRs in rf-SQUIDs[33] as well as in single Josephson junction[34] constructed on the surface of Bi_2Te_3. However, the location of gap closing, which is of key importance in braiding Majoranas for the purpose of quantum computation, still needs to be investigated.

In this paper, we report our investigations on the locations of gap closing as a function of magnetic flux in single Josephson junctions constructed on a Bi_2Te_3 surface. The results verify that the positions of gap closing, hence the Majoranas, can be manipulated by varying magnetic flux, in a manner proposed in our early studies.[33,34]

2. Experiment

Pb Josephson junction was fabricated on the surface of Bi_2Te_3 with five normal metal Pd electrodes distributed along the junction area to measure the local proximity induced minigap. The device was cooled down to 10 mK in a dilution refrigerator (Triton 200, Oxford Instruments) and measured by using lock-in amplifier technique. Fraunhofer diffraction pattern was measured with ac excitation current of 0.5 μA, and local contact resistance of Pd electrodes was measured by using a three-terminal measurement configuration.

3. Results and discussion

The devices used in this experiment contain single Josephson junction constructed on the surface of Bi_2Te_3, with normal-metal electrodes attached to the junction area to detect the local contact resistance. Figure 1(a) shows the scanning electron microscope (SEM) image of such a typical device. Two Pb electrodes separated by 1.35 μm were firstly fabricated on the surface of exfoliated Bi_2Te_3 flake of ∼100 nm in thickness. Then, over-exposed PMMA with evenly-spaced five windows of 600 nm in diameter was fabricated on the top of the Bi_2Te_3 surface and the Pb electrodes. Finally, Pd electrodes were deposited and contacted with the Bi_2Te_3 surface through the windows of the PMMA. For the device shown in Fig. 1(a), four of the five Pd electrodes worked well at low

*Project supported by the National Basic Research Program of China (Grant Nos. 2009CB929101 and 2011CB921702), the National Natural Science Foundation of China (Grant Nos. 91221203, 11174340, 11174357, 91421303, and 11527806), and the Strategic Priority Research Program B of the Chinese Academy of Sciences (Grant No. XDB07010100).

†Corresponding author. E-mail: lilu@iphy.ac.cn

© 2016 Chinese Physical Society and IOP Publishing Ltd

temperatures, labeled as A, B, C, and D. Electrodes A and B are located at the two ends of the junction. Electrodes C and D are located at 1/4 and 3/4 positions of the junction along the width direction.

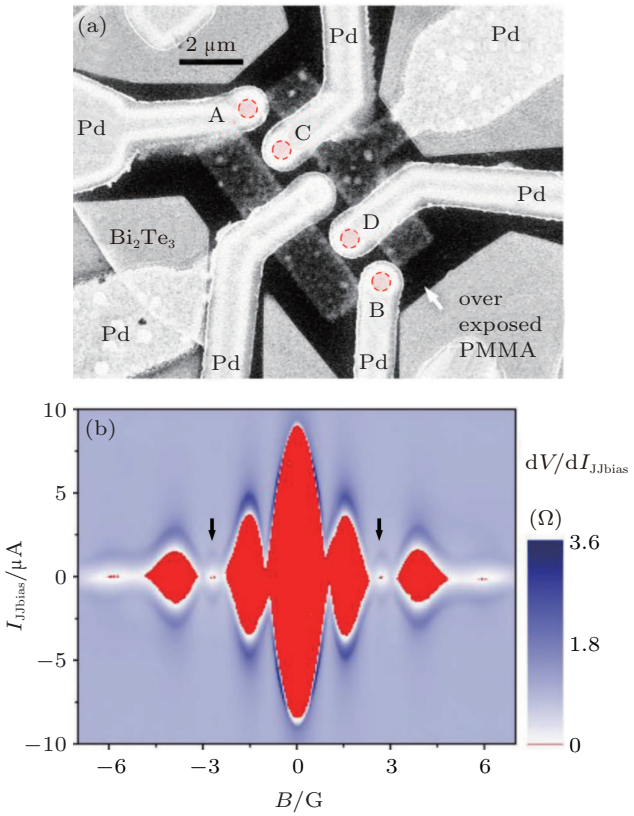


Fig. 1. (color online) (a) SEM image of a typical device used in this experiment, containing a Pb-Bi_2Te_3-Pb Josephson junction and five Pd electrodes connected to Bi_2Te_3 in the junction area. The black area is over-exposed PMMA to isolate the rest part of the Pd electrodes from touching the Pb films and the Bi_2Te_3 surface. (b) 2D plot of dV/dI_{JJbias} of the Josephson junction as a function of magnetic field and I_{JJbias}, the bias supercurrent of the Josepshon junction, showing a Fraunhofer-like pattern. The red color represents the zero-resistance state.

Figure 1(b) shows the 2D color plot of the differential resistance of Pb-Bi_2Te_3-Pb Josephson junction as a function of magnetic field B and bias current I_{JJbias} passing through the junction. The red-colored area represents the zero-resistance state (≤ 0.02 Ω). This demonstrates an equal-period oscillation, indicating that the Josephson junction is a large junction compared to the Josephson penetration depth, so that the supercurrent flows mostly near the two edges of the junction, interfering like in a dc SQUID. The oscillation period is $\Delta B = 1.3 \pm 0.3$ G, corresponding to an effective area of $S_{\rm eff} = \phi_0/\Delta B = 15.9$ μm^2 (where $\phi_0 = h/2e$ is flux quantum, e is the electron charge, and h is Planck's constant). This estimated area $S_{\rm eff}$ is in good agreement with the geometric area of the junction $6.7 \times 2.4 = 16.08$ μm^2 after considering flux compression (see the supplementary materials in Refs. [33] and [34].

The Josephson penetration depth of the device is[35] $\lambda_J = (4\pi e\mu_0 d j/h)^{-1/2} \approx 3.8$ μm, where μ_0 is the magnetic constant, d is the distance between the two Pb electrodes, $j = I_c/Wt$ is the supercurrent density, $I_c = 9$ μA is the critical supercurrent of the Josephson junction extracted from Fig. 1(b), $W = 6.7$ μm is the width of the junction, and $t \approx 100$ nm is the thickness of the Bi_2Te_3 flake. It can be seen that the λ_J is indeed less than the width of the junction, leading the junction to be marginally a large junction. The penetrated area defines a Fraunhofer-like envelope for the interference pattern, with the first node field located at ~2.3 G, as marked by the black arrows in Fig. 1(b).

The contact resistance between Pd electrodes and Bi_2Te_3 at positions A, B, C, and D was measured by using a three-terminal measurement configuration. Depending on detailed combination of the electrodes, the signal we measured might not only contain the contact resistance but also a part of the sample resistance. Nevertheless, the sample resistance was several orders of magnitude smaller than the contact resistance and thus its contribution could be neglected. Figs. 2(a)–2(d) show the 2D color plots of the contact resistance dV/dI_b measured at positions A, B, C, and D, respectively, as functions of magnetic field B and bias current I_b. Clear oscillations can be seen at all positions, with the same period as the Fraunhofer pattern shown in Fig. 1(b), indicating that the contact resistance is influenced by the EPR of the junction.

According to our previous studies,[33,34] the measured oscillations of the contact resistance reflect the oscillation of the superconducting minigap in Bi_2Te_3 beneath the Pd electrodes. According to the theory,[7] the energies of the Andreev bound states in a Josephson junction constructed on TI, including the lowest-energy bound states (i.e., the minigap), oscillate against the flux. We believe that the oscillation of contact resistance is caused by the oscillation of the minigap in Bi_2Te_3.

From Fig. 2 we see that the contact resistance that oscillates can either be suppressed (i.e., the whitish area in Figs. 2(a), 2(b), and 2(d)), or be enhanced (i.e., the dark-blue area in Fig. 2(c)). This is understandable within the Blonder–Tinkham–Klapwijk (BTK) theory.[36] When a normal-metal electrode is attached to the surface of a superconductor, the contact resistance within the gap energy can be either high or low depending on the interfacial barrier. In either case, the oscillation of the gap can be reflected on the contact resistance. From the data shown in Fig. 2, the size of the minigap in Bi_2Te_3 ranges from 20 to 50 μV, which is consistent with our previous observations on similar devices.[33,34] Apart from this, we notice from Figs. 2(b) and 2(d) that there is a zero-bias resistance peak which barely oscillates. This resistance peak can be more clearly seen from the vertical line cuts (Figs. 2(f) and 2(h)). It is likely caused by the reentrant resistance effect.[37]

Here we note that the current applied to the Pd electrodes for measuring the minigap are small enough in both the

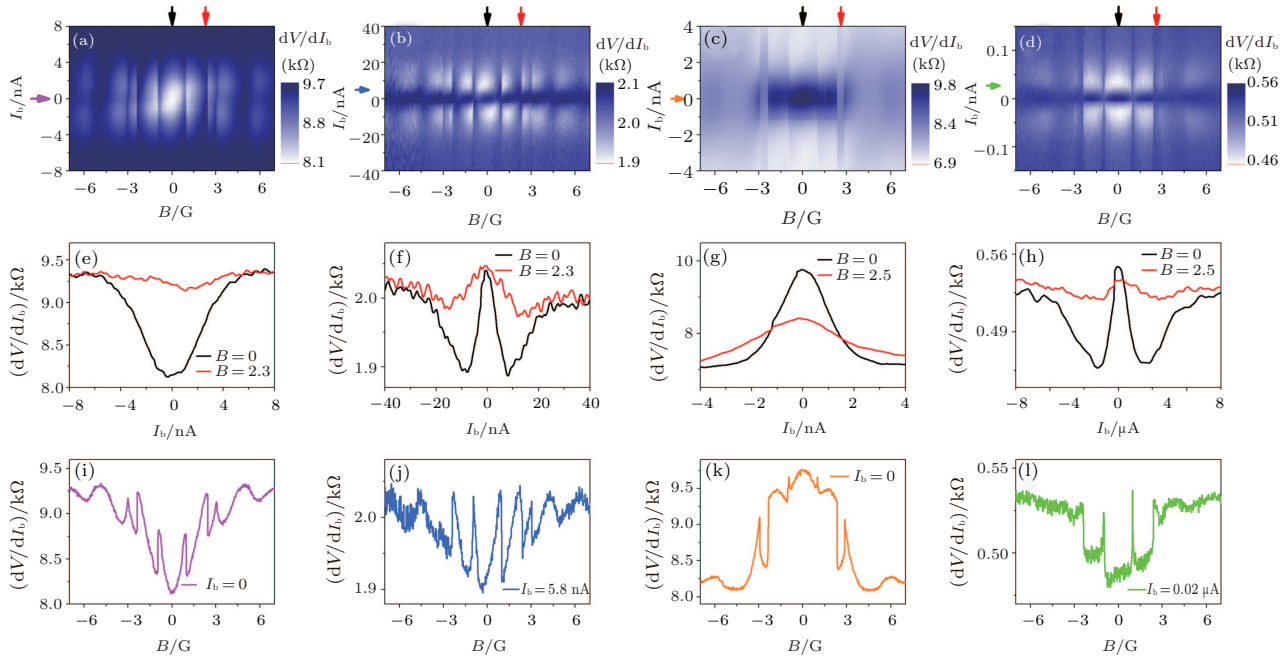


Fig. 2. (color online) (a)–(d) 2D color plots of the contact resistance dV/dI_b of positions A, B, C, and D, respectively, as functions of magnetic field and bias current, when $I_{JJbias} = 0$ and $T \approx 10$ mK. (e)–(h) The vertical line cuts in panels (a)–(d), respectively, at places marked by the arrows of the same color in corresponding color plots. The unit of the number in the legends is Gauss. (i)–(l) Horizontal line cuts in panels (a)–(d), respectively, at places marked by the arrows of the same color in corresponding color plots.

high- and low-contact resistance cases compared to the critical supercurrent of the Josephson junction. For position D whose contact resistance is much smaller than that of the other three Pd electrodes and thus the applied measuring current is relatively lager, the bias current I_b (≤ 0.15 μA) and the *ac* excitation current (5 nA for position *D*) were both much less than the critical supercurrent of the Josephson junction (9 μA). Such small probing current would not change the current or phase distribution of the Josephson junction and the minigap.

Figure 2 also shows that the contact resistance dV/dI_b at positions *A*, *B*, *C*, and *D* all jumps simultaneously at the node fields of the Fraunhofer pattern. The jump can be clearly seen at the horizontal line cuts shown in Figs. 2(i)–2(l). At positions *A* and *B*, dV/dI_b shows a fully skewed behavior, i.e., the minigap decreases gradually with varying field, and finally gets closed at the node fields of the Fraunhofer pattern, then jump abruptly to a pronounced value. The evolution of minigap against magnetic field can also be clearly seen from the vertical line cuts shown in Figs. 2(e) and 2(f). The red curves in these figures were taken at the fields indicated by the red arrows in the corresponding 2D color plots, showing nearly a gapless feature. The result is consistent with our previous finding.[34]

In contrast to the minigap at positions *A* and *B*, the minigap at positions *C* and *D* exhibits a step-like dependence against magnetic field, with jumps at the node fields of the Fraunhofer pattern, as shown in the 2D color plots (Figs. 2(c) and 2(d)) and the corresponding horizontal line cuts (Figs. 2(k) and 2(l)). The minigap fades out beyond the 2nd node of the Fraunhofer pattern. The red curves in Figs. 2(g) and 2(h) are the vertical line cuts taken at the fields indicated by the red arrows in the corresponding 2D color plots, demonstrating a relatively weak gap structure.

To calculate the minigap, we need to know the phase difference of the Josephson junction. When $I_{JJbias} = 0$, the local phase difference can be written as[33,34]

$$\varphi(B,x) = 2\pi\alpha\frac{xHB}{\phi_0} \pm \pi \mathrm{int}\left(\frac{\phi}{\phi_0}\right), \tag{1}$$

where x is defined from $-W/2$ to $W/2$, H is the effective junction length after considering flux compression (see the supplementary materials in Refs. [33] and [34]), and ϕ is the flux in the junction. The first term is the phase difference determined by the flux in the junction area, and the second term represents an additional π phase shift whenever the flux reaches the nodes of the Fraunhofer pattern. The mechanism of the π phase shift is explained elsewhere.[34]

Figures 3(a)–3(c) show the phase distribution lines of the junction near the first, the second, and the third node of the Fraunhofer pattern, respectively. The gray arrows indicate the expected π phase shift of the phase distribution lines near the nodes of Fraunhofer pattern.[34] The red circles represent the position where $\varphi(x)$ reaches odd multiples of π, so that the local minigap is expected to be closed. With the variation of flux in the junction area, the phase distribution line rotates about the center of the junction, resulting in the change of the minigap as well as the motion of the gap-closing points in the junction. It can be seen that the minigap at the center of the junction is unchanged with varying flux (the minigap is either

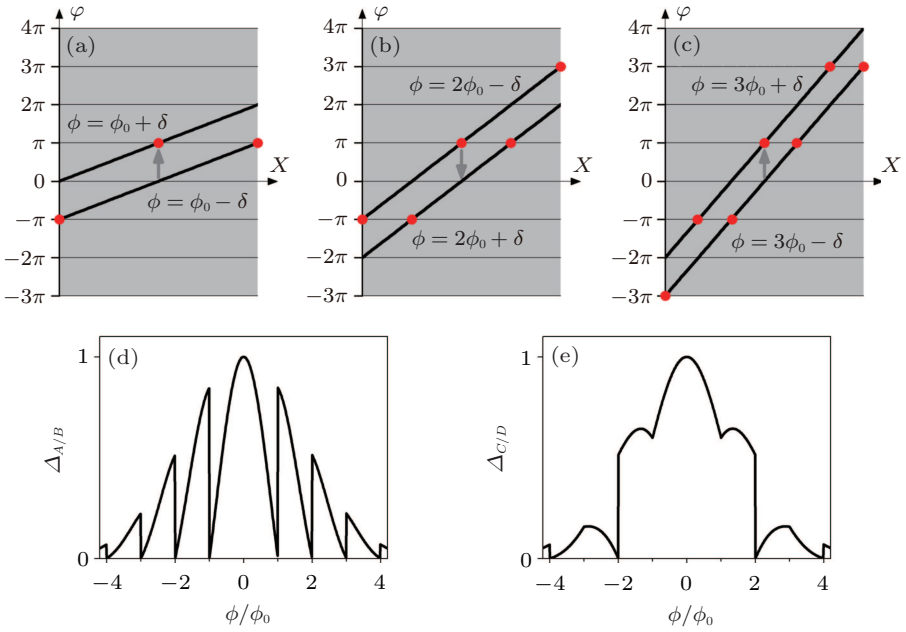


Fig. 3. (color online) (a)–(c) The phase distribution of the junction as a function of position x before/after the jumping when the flux in the junction reaches ϕ_0, $2\phi_0$, and $3\phi_0$, respectively. The phase distribution lines undergo π phase shift, as indicated by the gray arrows. The red circles represent the place where the local $\varphi(x)$ hits odd multiples of π so that the minigap is closed. (d) The calculated minigap Δ at position A/B (i.e., at $x = \pm W/2$). (e) The calculated Δ at position C/D (i.e., at $x = \pm W/4$).

maximized or close). At positions A and B ($x = \pm W/2$), $\varphi(x)$ reaches odd multiples of π at every node of the Fraunhofer pattern. At positions C and D ($x = \pm W/4$), $\varphi(x)$ reaches π only beyond the second node of the Fraunhofer pattern.

It is known that the minigap is defined by the energy separation between the two lowest-energy Andreev bound state, the latter has the form of:[38,39] $E_n = \pm\Delta_0[1 - D_0 \sin^2(\varphi/2)]^{1/2}$, where E_n and D_n are the energy and transmission coefficient of the n^{th} mode of quasiparticles, respectively. As has been pointed out,[33,34] the time-reversal symmetry protected helical surface states are immune from backscattering, leading to the full transparency (i.e., $D_n = 1$) and the appearance of topologically-protected perfect Andreev reflection. In this case, the minigap can be fully closed and described by the following expression:

$$\Delta \propto |\cos(\varphi/2)|. \tag{2}$$

Figures 3(d) and 3(e) show the calculated minigap at positions A/B and C/D, respectively, by using Eqs. (1) and (2). Since the strength of the minigap decays with magnetic field, in these two figures we have phenomenologically imposed a Gaussian-like envelope $e^{-\gamma(\phi/\phi_0)^2}$ (where $\gamma = 0.2$) for the minigap. The results excellently mimic the data shown in Fig. 2. This confirms that the Josephson junctions constructed on TI surface are indeed fully transparent to quasiparticle transport so that Majoranas can be hosted, and that the gap-closing points in the junction, where Majoranas are supposed to be held, can be predicted and manipulated by varying magnetic flux via the formulas listed above.

For topologically-trivial states such as the bulk states of Bi_2Te_3, their Andreev bound states are located at relatively higher energies compared to that of the topologically-nontrivial surface states, thus will not influence the process of minigap closing.

We note that the observed gap closing is often incomplete. This is because that the minigap closes completely only at certain x coordinates precisely, whereas the local Pd electrodes used to detect gap closing has a finite size (600 nm in diameter).[33] Position uncertainty of gap closing caused by thermal smearing at $\sim$10 mK places additional difficulty to align the Pd electrodes to the gap-closing points.[33]

4. Conclusion

To conclude, we have measured the local minigap in single Josephson junctions constructed on Bi_2Te_3 surface, as a function of position x and magnetic flux. Gap closing is observed and can only be explained within the scenario that the quasiparticle transport is fully transparent in the junction area. The results support the theoretical proposals that Majorana zero modes can be hosted in Josephson junctions constructed on the TI surface. Our results further verify that the places of gap closing can be predicted by using Eqs. (1) and (2), based on which future braiding of Majorana fermions could be designed.

Acknowledgment

We would like to thank L Fu, Z Fang, X Dai, T Xiang, X C Xie, Q F Sun, R Du, G M Zhang and X Hu for fruitful

discussions.

References

[1] Majorana E 1937 *Nuovo Cimento* **14** 171
[2] Wilczek F 2009 *Nat. Phys.* **5** 614
[3] Service R F 2011 *Science* **332** 193
[4] Franz M 2010 *Physics* **3** 24
[5] Franz M 2013 arXiv:1302.3641v1
[6] Read N and Green D 2000 *Phys. Rev. B* **61** 10267
[7] Fu L and Kane C L 2008 *Phys. Rev. Lett.* **100** 096407
[8] Oreg Y, Refael G and von Oppen F 2010 *Phys. Rev. Lett.* **105** 177002
[9] Mourik V, Zuo K, Frolov S M, Plissard S R, Bakkers E P A M and Kouwenhoven L P 2012 *Science* **336** 1003
[10] Deng M T, Yu C L, Huang G Y, Larsson M, Caroff P and Xu H Q 2012 *Nano Lett.* **12** 6414
[11] Das A, Ronen Y, Most Y, Oreg Y, Herblum M and Shtrikman H 2012 *Nat. Phys.* **8** 887
[12] Churchill H O H, Fatemi V, Grove-Rasmussen K, Deng M T, Caroff P, Xu H Q and Marcus C M 2013 *Phys. Rev. B* **87** 241401
[13] Finck A D K, Van Harlingen D J, Mohseni P K, Jung K and Li X 2013 *Phys. Rev. Lett.* **110** 126406
[14] Nadj-Perge S, Drozdov I K, Li J, Chen H, Jeon S, Seo J, MacDonald A H, Bernevig B A and Yazdani A 2014 *Science* **346** 602
[15] Sasaki S, Kriener M, Segawa K, Yada K, Tanaka Y, Sato M and Ando Y 2011 *Phys. Rev. Lett.* **107** 217001
[16] Yang F, Ding Y, Qu F, Shen J, Chen J, Wei Z, Ji Z, Liu G, Fan J, Yang C, Xiang T and Lu L 2012 *Phys. Rev. B* **85** 104508
[17] Rokhinson L P, Liu X and Furdyna J K 2012 *Nat. Phys.* **8** 795
[18] Kurter C, Finck A D K, Ghaemi P, Hor Y S and Van Harlingen D J 2014 *Phys. Rev. B* **90** 014501
[19] Kurter C, Finck A D K, Hor Y S and Van Harlingen D J 2015 *Nat. Commun.* **6** 7130
[20] Hart S, Ren H, Wagner T, Leubner P, Mühlbauer M, Brüne C, Buhmann H, Molenkamp L W and Yacoby A 2014 *Nat. Phys.* **10** 638
[21] Pribiag V S, Beukman A J, Qu F, Cassidy M C, Charpentier C, Wegscheider W and Kouwenhoven L P 2015 *Nat. Nano.* **10** 593
[22] Sochnikov I, Maier L, Watson C A, Kirtley J R, Gould C, Tkachov G, Hankiewicz E M, Brüne C, Buhmann H, Molenkamp L W and Moler K A 2015 *Phys. Rev. Lett.* **114** 066801
[23] Wiedenmann J, Bocquillon E, Deacon R S, Hartinger S, Herrmann O, Klapwijk T M, Maier L, Ames C, Brüne C, Gould C, Oiwa A, Ishibashi K, Tarucha S, Buhmann H and Molenkamp L W 2016 *Nat. Commun.* **7** 10303
[24] Potter A C and Fu L 2013 *Phys. Rev. B* **88** 121109
[25] Yu Kitaev A 2011 *Phys. Usp.* **44** 131
[26] Kwon H J, Sengupta K and Yakovenko V M 2004 *Low Temp. Phys.* **30** 613
[27] Fu L and Kane C L 2009 *Phys. Rev. B* **79** 161408
[28] Lutchyn R M, Sau J D and Das Sarma S 2010 *Phys. Rev. Lett.* **105** 077001
[29] Diez M, Fulga I C, Pikulin D I, Wimmer M, Akhmerov A R and Beenakker C W J 2013 *Phys. Rev. B* **87** 125406
[30] Beenakker C W J, Pikulin D I, Hyart T, Schomerus H and Dahlhaus J P 2013 *Phys. Rev. Lett.* **110** 017003
[31] Wieder B J, Zhang F and Kane C L 2014 *Phys. Rev. B* **89** 075106
[32] Lee S P, Michaeli K, Alicea J and Yacoby A 2014 *Phys. Rev. Lett.* **113** 197001
[33] Pang Y, Shen J, Qu F, Wang J, Feng J, Fan J, Liu G, Ji Z, Jing X, Yang C, Sun Q, Xie X C, Fu L and Lu L 2015 arXiv:1503.00838v2
[34] Pang Y, Wang J, Lyu Z, Yang G, Fan J, Liu G, Ji Z, Jing X, Yang C and Lu L 2016 arXiv:1603.04540
[35] Barone A 1982 *Physics and Application of the Josephson Effect* (New York: John Wiley and Sons)
[36] Blonder G E, Tinkham M and Klapwijk M T 1982 *Phys. Rev. B* **25** 4515
[37] Finck A D K, Kurter C, Hor Y S and Van Harlingen D J 2014 *Phys. Rev. X* **4** 041022
[38] Golubov A A, Kupriyanov M Y and Il'ichev E 2004 *Rev. Mod. Phys.* **76** 411
[39] Beenakker C W J 1992 *Transport Phenomena in Mesoscopic Systems* (Berlin: Fukuyama H and Ando T)